Int. J. of Applied Mechanics and Engineering, 2017, vol.22, No.3, pp.697-715
DOI: 10.1515/ijame-2017-0044

CURVILINEAR SQUEEZE FILM BEARING LUBRICATED WITH A DEHAVEN FLUID OR WITH SIMILAR FLUIDS

A. WALICKA*, P. JURCZAK and J. FALICKI
University of Zielona Góra, Faculty of Mechanical Engineering
ul. Szafrana 4, 65-516 Zielona Góra, POLAND
E-mails: A.Walicka@ijame.uz.zgora.pl
P.Jurczak@ibem.uz.zgora.pl
J.Falicki@ibem.uz.zgora.pl

In the paper, the model of a DeHaven fluid and some other models of non-Newtonian fluids, in which the shear strain rates are known functions of the powers of shear stresses, are considered. It was demonstrated that these models for small values of material constants can be presented in a form similar to the form of a DeHaven fluid. This common form, called a unified model of the DeHaven fluid, was used to consider a curvilinear squeeze film bearing. The equations of motion of the unified model, given in a specific coordinate system are used to derive the Reynolds equation. The solution to the Reynolds equation is obtained by a method of successive approximations. As a result one obtains formulae expressing the pressure distribution and load-carrying capacity. The numerical examples of flows of the unified DeHaven fluid in gaps of two simple squeeze film bearings are presented.

Key words: DeHaven fluid, modified Reynolds equation, squeeze film, mechanical parameters of the bearing.

1. Introduction

Viscosity of lubricating oils increases with the additives concentration and it is relatively independent of temperature and usually exhibits a non-linear relation between the shear stress and the rate of shear in a shear flow. There has been no generally acceptable theory taking into account the flow behaviour of non-Newtonian lubricants. Studies have been done on fluid film lubrication employing several models such as micropolar (see e.g.,: Walicka, [1]) couple-stress (Walicki and Walicka [2]), mixture (Khonsari and Dai [3]), viscoplastic (Lipscomb and Denn [4]; Dorier and Tichy [5]), pseudo-plastic (Wada and Hayashi [6]; Swamy *et al*. [7]; Rajalingham *et al*. [8]). Naturally, this list is not complete and given only to present the possibility of mathematical modelling. A more complete list may be found in (Walicka [9]; Walicki [10]).

In recent years, tribologists have done a great deal of work on pseudo-plastic lubricants; the viscosity of these kinds of lubricants displays a non-linear relationship between the shear stress and the shear strain rate. There are many known formulae to model this relationship. One of the first was power-series development and in consequence polynomials were suggested. The polynomial given by Kraemer and Wiliamson [11], which was later independently proposed by Rabinowitsch [12] should be cited here. In the sixties of the past century Rotem and Shinnar [13] returned to the polynomial representation proposing their own model similar to that one of Rabinowitsch.

Theoretical considerations and some experiments carried out by Wada and Hayashi [6] indicated the usefulness of the Rabinowitsch fluid to modelling various lubrication problems. These problems have been analyzed by many investigators, for instance journal bearings were studied by Wada and Hayashi [6], Rajalingham *et al*. [8], Sharma *et al.* [14], Swamy *et al.* [7], hydrostatic thrust bearing by a Singh *et al.* [15], squeeze film bearings by Hashimoto and Wada [16], Lin [17], Lin *et al.* [18]. More general lubrication

* To whom correspondence should be addressed

problems include hybrid bearings modelled by two generally non-coaxial surfaces of revolution which can work simultaneously as journal and/or thrust bearings. Some theoretical considerations about these bearings may be found in the works by Walicka *et al.* [19, 20], Ratajczak *et al.* [21], Walicka and Walicki [22]; these authors considered both externally pressurized bearings with and without rotational inertia and squeeze film bearings lubricated with a Rotem-Shinnar fluid. From the results of all the papers referred to above, it follows that the pseudo-plastic lubricants properties affect the bearing performance significantly.

This paper is mainly concerned with the non-Newtonian effects in the squeeze film bearing lubricated with a DeHaven fluid whose one dimensional model is given as follows [23]

$$\mu_0\dot{\gamma} = \tau\left(1 + k|\tau|^n\right) \tag{1.1}$$

where k is an empirical constant determined from experiments.
Let us consider – for example – two other models of pseudoplastic fluids, namely:

– Ree-Eyring fluid [24]

$$\tau = \mu_0\dot{\gamma}\left[\frac{\sinh(k\tau)}{k\tau}\right]^{-1}, \tag{1.2}$$

– Meter fluid [25]

$$\tau = \left[\mu_\infty + \frac{\mu_0 - \mu_\infty}{1 + (k\tau)^n}\right]\dot{\gamma}. \tag{1.3}$$

In lubrication technology one uses only such fluids for which the material constants are small and which satisfy the relationship

$$k\tau < 1;$$

the above model equations in series forms can be presented as follows, respectively

$$\tau = \frac{\mu_0\dot{\gamma}}{\left[1 + \frac{(k\tau)^2}{3!} + \frac{(k\tau)^4}{5!} + \ldots\right]}, \tag{1.4}$$

$$\tau = \mu_0\dot{\gamma}\left[1 - \frac{\mu}{\mu_0}(k\tau)^n + \frac{\mu}{\mu_0}(k\tau)^{2n} - \ldots\right], \qquad \mu = \mu_0 - \mu_\infty. \tag{1.5}$$

For a sufficiently small value of $(k\tau)$ it is enough to limit the expression in brackets of Eqs (1.4) and (1.5) to the first two terms; then they will be, respectively

$$\mu_0\dot{\gamma} = \tau\left(1 + \frac{k^2}{6}\tau^2\right), \tag{1.6}$$

$$\mu_0\dot{\gamma} = \tau\left(1 + \frac{\mu k^n}{\mu_0}\tau^n\right). \tag{1.7}$$

Table 1. Models of fluids similar to the DeHaven fluid model.

No	Author(s)	Original model	Model taken into account	k_i	Comments
$n_i = n$					"$n+1$" power models
1	DeHaven	$\mu_0\dot{\gamma} = \tau\left(1 + k\lvert\tau\rvert^n\right)$	–	k	
2	Meter	$\tau = \left[\mu_\infty + \frac{\mu_0 - \mu_\infty}{1 + (k\tau)^n}\right]\dot{\gamma}$	$\mu_0\dot{\gamma} = \tau\left(1 + \frac{\mu k^n}{\mu_0}\tau^n\right)$	$\frac{\mu k^n}{\mu_0}$	$\mu = \mu_0 - \mu_\infty$
$n_i = n-1$					"n" power model
3	Ellis	$\tau = \frac{\mu_0\dot{\gamma}}{1 + k\lvert\tau\rvert^{n-1}}$	$\mu_0\dot{\gamma} = \tau\left(1 + k\lvert\tau\rvert^{n-1}\right)$	k	
$n_i = 2$					"Cubic" models
4	Rotem-Shinnar	$\tau = \frac{\mu_0\dot{\gamma}}{1 + \sum_i^n k_i\tau^{2i}}$	$\mu_0\dot{\gamma} = \tau\left(1 + k\tau^2\right)$	k	The model has a practical meaning for $i = 1$
5	Ree-Eyring	$\tau = \mu_0\dot{\gamma}\left[\frac{\sinh(k\tau)}{k\tau}\right]^{-1}$	$\mu_0\dot{\gamma} = \tau\left(1 + \frac{k^2}{6}\tau^2\right)$	$\frac{k^2}{6}$	
6	Rabinowitsch	$\tau = \frac{\mu_0\dot{\gamma}}{1 + k\tau^2}$	$\mu_0\dot{\gamma} = \tau\left(1 + k\tau^2\right)$	k	
7	Reiner-Philippoff	$\tau = \left[\mu_\infty + \frac{\mu_0 - \mu_\infty}{1 + (k\tau)^2}\right]\dot{\gamma}$	$\mu_0\dot{\gamma} = \tau\left(1 + \frac{\mu k^2}{\mu_0}\tau^2\right)$	$\frac{\mu k^2}{\mu_0}$	$\mu = \mu_0 - \mu_\infty$
$n_i = 1$					"Quadratic" models
8	Peek-McLean	$\tau = \left[\mu_\infty + \frac{\mu_0 - \mu_\infty}{1 + (k\tau)}\right]\dot{\gamma}$	$\mu_0\dot{\gamma} = \tau\left(1 + \frac{\mu k}{\mu_0}\tau\right)$	$\frac{\mu k}{\mu_0}$	$\mu = \mu_0 - \mu_\infty$
9	Seely	$\tau = \left[\mu_\infty + \frac{\mu_0 - \mu_\infty}{e^{(k\tau)}}\right]\dot{\gamma}$	$\mu_0\dot{\gamma} = \tau\left(1 - \frac{\mu k}{\mu_0}\tau\right)$	$-\frac{\mu k}{\mu_0}$	$\mu = \mu_0 - \mu_\infty$

Let us consider the other similar models of pseudoplastic fluids given in the second column of Table 1 [23-30]. Taking into account the forms of these models given in the third column of Table 1 one can present them in a simple unified form

$$\mu_0\dot{\gamma} = \tau\left(1 + k_i\lvert\tau\rvert^{n_i}\right); \tag{1.8}$$

the material coefficients k_i and n_i are also given in Tab.1. Here Eq.(1.8) is so called constitutive equation of the DeHaven fluid. In an experimental research by Wada and Hayashi [6], a range of μ_0 and k_i (in the case of the Rabinowitsch fluid for which $n_i = 2$) for various working conditions of lubricants with additives has been determined. It results from this research that the values of k_i may be: $k_i < 0$ or $k_i > 0$; if $k_i = 0$, then Eq.(1.8) describes a Newtonian fluid

2. Equations of motion of the unified DeHaven fluid model

The general equations of motion of a viscous fluid in a three-dimensional form are as follows:

– equation of continuity

$$\operatorname{div}\mathbf{v} = 0\,, \tag{2.1}$$

– equation of momentum

$$\rho\frac{d\mathbf{v}}{dt} = \operatorname{div}\boldsymbol{T}\,, \qquad \boldsymbol{T} = -p\boldsymbol{1} + \boldsymbol{\Lambda} \tag{2.2}$$

or

$$\rho\frac{d\mathbf{v}}{dt} = -\nabla p + \operatorname{div}\boldsymbol{\Lambda}\,; \tag{2.3}$$

here the constitutive Eq.(1.8) takes the form

$$\mu_0\boldsymbol{A}_1 = \boldsymbol{\Lambda}\left(1 + k_i|\Lambda|^{n_i}\right), \qquad \Lambda = \left[\frac{1}{2}\operatorname{tr}\left(\boldsymbol{\Lambda}^2\right)\right]^{1/2} \tag{2.4}$$

and p is the pressure, $\boldsymbol{1}$ is the unit tensor, Λ is the second invariant of the extra stress tensor $\boldsymbol{\Lambda}$, $\boldsymbol{A}_1$ is the first Rivlin-Ericksen stretching tensor defined by

$$\boldsymbol{A}_1 = \boldsymbol{L} + \boldsymbol{L}^T\,, \qquad \boldsymbol{L} = \operatorname{grad}\mathbf{v} \tag{2.5}$$

$\mathbf{v}$ is the velocity vector and T denotes the transposition.

Let us consider a thrust bearing with a curvilinear profile of the working surfaces shown in Fig.1. The lower fixed surface is described by the function $R(x)$ which denotes the radius of this surface. The bearing clearance thickness is given by the function $h(x,t)$.

An intrinsic curvilinear orthogonal coordinate system x, ϑ, y linked with the lower bearing surface is also presented in Fig.1.

The physical parameters of the Prandtl fluid flow are the velocity components υ_x, υ_y, pressure p. With regard to the axial symmetry of the flow these parameters are not dependent on the angle ϑ.

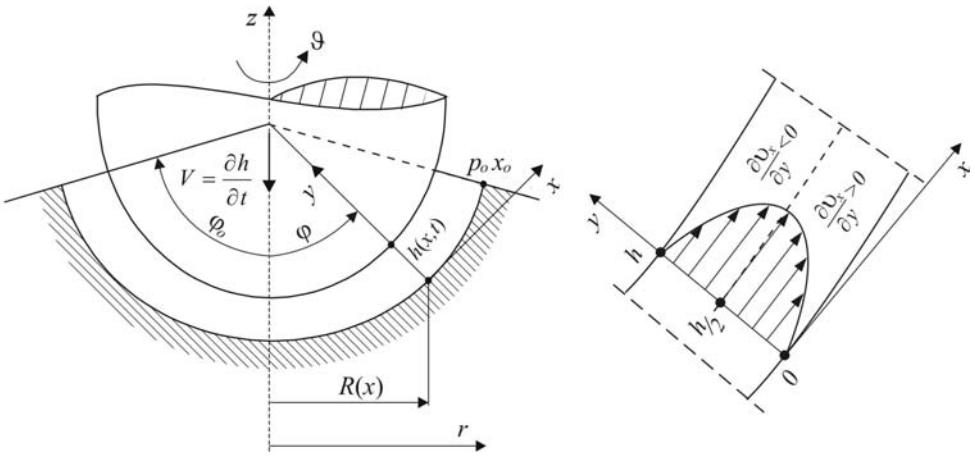

Fig.1. Geometry of a curvilinear bearing.

The assumption typical for the flow in a narrow gap (Walicka [2], Walicki [3])

$$h(x,t) << R(x), \qquad \upsilon_y << \upsilon_x, \qquad \frac{\partial}{\partial x} << \frac{\partial}{\partial y}$$

can be used to make order-of-magnitude arguments for Eqs (2.3)-(2.5).

A further simplification comes by noting – in accordance with the lubrication approximation – that the modified Reynolds number R_λ is very small

$$R_\lambda = \frac{h_0}{l_0}\mathrm{Re} << 1$$

and the inertia effects are also very small; here Re is the classic Reynolds number, h_0 is the characteristic bearing gap thickness, l_0 is the characteristic bearing gap length.

If some asymptotic transformations are made, the same as in (Walicka [2], Walicki [3]) these equations can be reduced to a simpler form [31, 32]

$$\frac{1}{R}\frac{\partial(R\upsilon_x)}{\partial x} + \frac{\partial \upsilon_y}{\partial y} = 0, \tag{2.6}$$

$$\frac{\partial p}{\partial x} = \frac{\partial \Lambda_{yx}}{\partial y}, \tag{2.7}$$

$$0 = -\frac{\partial p}{\partial y}. \tag{2.8}$$

The last equation yields

$$p = p(x,t). \tag{2.9}$$

The constitutive Eq.(2.4) now takes the form

$$\mu_0 \frac{\partial \upsilon_x}{\partial x} = \Lambda_{yx}\left(1 + k_i\left|\Lambda_{yx}\right|^{n_i}\right). \tag{2.10}$$

The problem statement is complete after specification of boundary conditions. These conditions for the velocity components are stated as follows

$$\upsilon_x(x,0,t) = 0, \qquad \upsilon_x(x,h,t) = 0, \tag{2.11}$$

$$\upsilon_y(x,0,t) = 0, \qquad \upsilon_y(x,h,t) = \frac{\partial h}{\partial t} = \dot{h}; \tag{2.12}$$

the boundary conditions for the pressure distribution will be presented in the next section.

3. Solution to the equations of motion

Integrating Eq.(2.7) with respect to *y,* we have

$$\Lambda_{yx} = C_1 + y\frac{\partial p}{\partial x}. \tag{3.1}$$

Putting this equation in Eq.(2.10) ,we obtain

$$\mu_0 \frac{\partial \upsilon_x}{\partial y} = \left(C_1 + y\frac{\partial p}{\partial x} \right) \left[1 + k_i \left| C_1 + y\frac{\partial p}{\partial x} \right|^{n_i} \right]. \tag{3.2}$$

Assuming the flow symmetry with respect to the gap median surface, we have (see: Fig.1)

$$\left. \frac{\partial \upsilon_x}{\partial y} \right|_{y=\frac{h}{2}} = 0$$

then

$$\left(C_1 + \frac{h}{2}\frac{\partial p}{\partial x} \right) \left[1 + k_i \left| C_1 + \frac{h}{2}\frac{\partial p}{\partial x} \right|^{n_i} \right] = 0.$$

Note that the unique real root of this equation is equal to

$$C_1 = -\frac{h}{2}\frac{\partial p}{\partial x}. \tag{3.3}$$

Introducing (3.3) into Eq.(3.2) one obtains

$$\frac{\partial \upsilon_x}{\partial y} = \frac{2y-h}{2\mu_0}\left(\frac{\partial p}{\partial x} \right) + \frac{k_i}{\mu_0} \left| \frac{2y-h}{2} \left(\frac{\partial p}{\partial x} \right) \right|^{n_i+1} \tag{3.4}$$

the equation whose integral – after satisfying the boundary conditions (2.11) – is equal to

$$\upsilon_x = \frac{1}{2\mu_0} \left[\left(\frac{h}{2} \right)^2 - \left(\frac{2y-h}{2} \right)^2 \right] \left(-\frac{\partial p}{\partial x} \right) + \frac{k_i}{\mu_0 (n_i+2)} \left[\left(\frac{h}{2} \right)^{n_i+2} - \left| \frac{2y-h}{2} \right|^{n_i+2} \right] \left(-\frac{\partial p}{\partial x} \right)^{n_i+1}. \tag{3.5}$$

To find the equation for the determination of the pressure distribution let us return to the equation of continuity (2.1). Introducing in Eq.(2.1) the flow velocity given by Eq.(3.5) and making the integration across the gap thickness we will obtain the following form of the Reynolds equation

$$\frac{1}{R}\frac{\partial}{\partial x} Rh^3 \left[\left(\frac{\partial p}{\partial x} \right) - \frac{3k_i h^{n_i}}{2^{n_i}(n_i+3)} \left(-\frac{\partial p}{\partial x} \right)^{n_i+1} \right] = 12\mu_0 \frac{\partial h}{\partial t}. \tag{3.6}$$

This is a non-linear equation whose solution may be presented (in the first approximation) in the form of a sum

$$p = p^{(0)} + p^{(1)}. \tag{3.7}$$

Assuming that $p^{(0)} >> p^{(1)}$ and substituting Eq.(3.7) into Eq.(3.6) ,we arrive at two linearized equations:

- the first one

$$\frac{1}{R}\frac{\partial}{\partial x}Rh^3\frac{\partial p^{(0)}}{\partial x}=12\mu_0\frac{\partial h}{\partial t}, \tag{3.8}$$

- and the other

$$\frac{1}{R}\frac{\partial}{\partial x}Rh^3\frac{\partial p^{(1)}}{\partial x}=\frac{1}{R}\frac{\partial}{\partial x}\frac{3k_iRh^{n_i+3}}{2^{n_i}\left(n_i+3\right)}\left(-\frac{\partial p^{(0)}}{\partial x}\right)^{n_i+1}. \tag{3.9}$$

The boundary conditions for the pressure are

$$\left.\frac{\partial p^{(0)}}{\partial x}\right|_{x=0}=0, \qquad p^{(0)}\left(x_o,t\right)=p_o, \tag{3.10}$$

$$\left.\frac{\partial p^{(1)}}{\partial x}\right|_{x=0}=0, \qquad p^{(1)}\left(x_o,t\right)=0. \tag{3.11}$$

The solution of Eqs (3.8) and (3.9) are given, as follows

$$p\left(x,t\right)=p_o-12\mu_0\left[F_o^{(n_i)}-F^{(n_i)}\left(x,t\right)\right] \tag{3.12}$$

where

$$F^{(n_i)}\left(x,t\right)=I\left(x,t\right)+\frac{k_i\left(6\mu_0\right)^{n_i+1}}{2\mu_0\left(n_i+3\right)}J^{(n_i)}\left(x,t\right), \qquad F_o^{(n_i)}=F^{(n_i)}\left(x_o,t\right),$$

$$I\left(x,t\right)=\int\frac{\int R\dot{h}dx}{Rh^3}dx, \qquad J^{(n_i)}\left(x,t\right)=\int\frac{\left(-\int R\dot{h}dx\right)^{n_i+1}}{R^{n_i+1}h^{2n_i+3}}dx, \qquad \dot{h}=\frac{\partial h}{\partial t}. \tag{3.13}$$

The load-carrying capacity is defined by

$$N=2\pi\int_0^{x_o}\left(p-p_o\right)R\cos\varphi dx\,; \tag{3.14}$$

the sense of the angle φ arises from Fig.1.

Note that $I\left(x,t\right)$ represents a Newtonian pressure distribution in the squeeze film while $J^{(n_i)}\left(x,t\right)$ is a pseudoplastic correction to this pressure.

4. Squeeze film in a radial thrust bearing

Let us consider a radial thrust bearing with a squeezed film of the DeHaven lubricant modelled by two parallel disks (Fig.2).

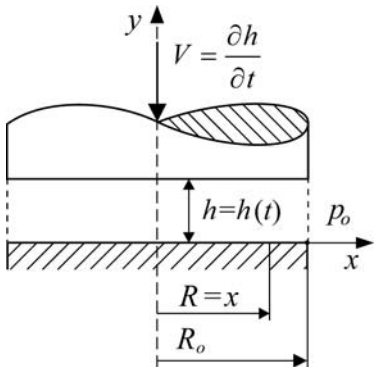

Fig.2. Squeeze film in a radial thrust bearing.

Introducing the following parameters

$$R = x\,, \qquad \tilde{R} = \tilde{x} = \frac{x}{x_o}\,, \qquad \tilde{h} = \frac{h}{h_o} = e(t), \qquad e(t) = 1 - \varepsilon(t)\,, \qquad \dot{\varepsilon} = \frac{d\varepsilon}{dt}\,, \tag{4.1}$$

$$\tilde{p} = \frac{(p - p_o)}{\mu\dot{\varepsilon}}\left(\frac{h_o}{x_o}\right)^2, \qquad \tilde{N} = \frac{N}{\mu\dot{\varepsilon}x_o^2}\left(\frac{h_o}{x_o}\right)^2, \qquad \lambda^{(n_i)} = k_i\left(\frac{\mu_0\dot{\varepsilon}x_o}{h_o}\right)^{n_i},$$

we will obtain the formulae for the dimensionless pressure distribution and load-carrying capacity for the radial thrust bearing with a squeeze film of the lubricant

$$\tilde{p} = \frac{3}{e^3}\left[\left(1-\tilde{x}^2\right) - \frac{2\cdot 3^{n_i+1}}{(n_i+2)(n_i+3)}\frac{\lambda^{(n_i)}}{e^{2n_i}}\left(1-\tilde{x}^{n_i+2}\right)\right], \tag{4.2}$$

$$\tilde{N} = \frac{3\pi}{2e^3}\left[1 - \frac{4\cdot 3^{n_i+1}\lambda^{(n_i)}}{(n_i+3)(n_i+4)e^{2n_i}}\right]. \tag{4.3}$$

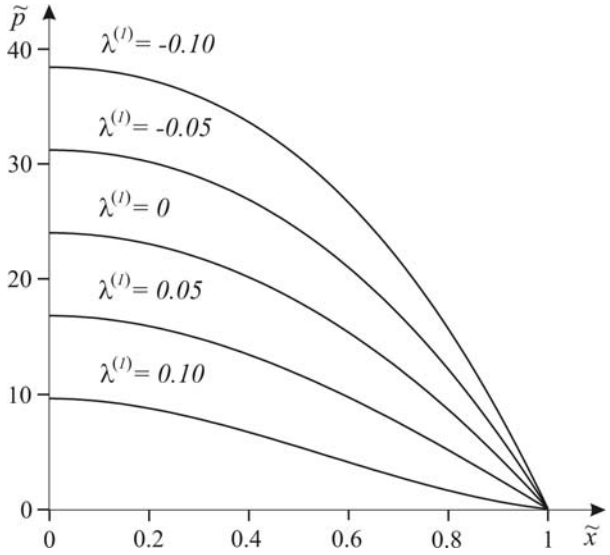

Fig.3. Dimensionless pressure distribution in the radial squeeze film bearing for $\varepsilon = 0.5$ versus different values of $\lambda^{(1)}$ for $n_i = 1$ (the case of the Peek-McLean type lubricant).

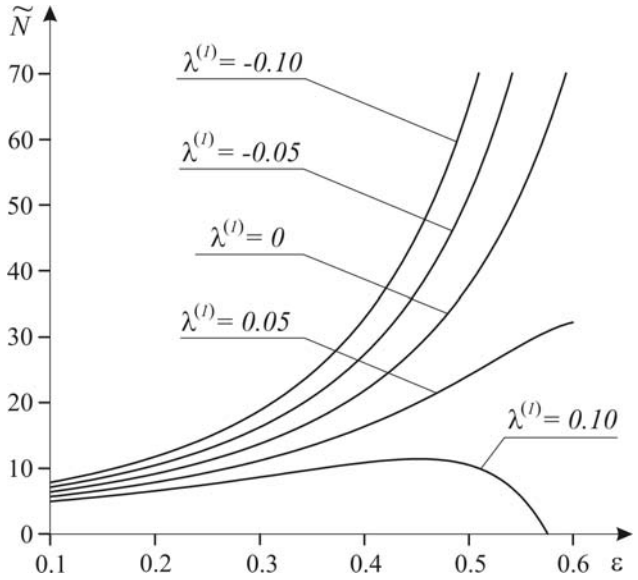

Fig.4. Dimensionless load-carrying capacity in the radial squeeze film bearing for different values of $\lambda^{(1)}$ for $n_i = 1$ (the case of the Peek-McLean type lubricant).

The plots of the dimensionless pressure distribution and load-carrying capacity are presented in Figs 3 and 4 for the Peek-McLean fluid for which $n_i = 1$, in Figs 5 and 6 for one of the fluids which represent the group of cubic models (e.g.: the Rabinowitsch fluid) where $n_i = 2$ and in Figs 7 and 8 for one of the fluids near the group of DeHaven-Ellis models where $n_i = 3$.

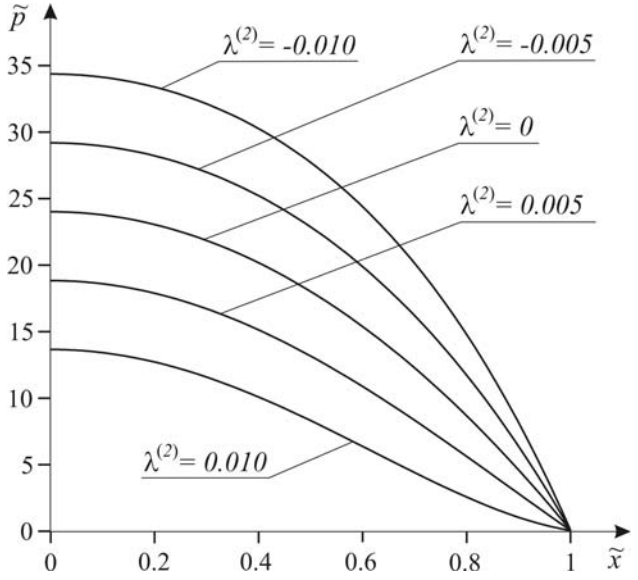

Fig.5. Dimensionless pressure distribution in the radial squeeze film bearing for $\varepsilon = 0.5$ versus different values of $\lambda^{(2)}$ for $n_i = 2$ (the case of the cubic type lubricant).

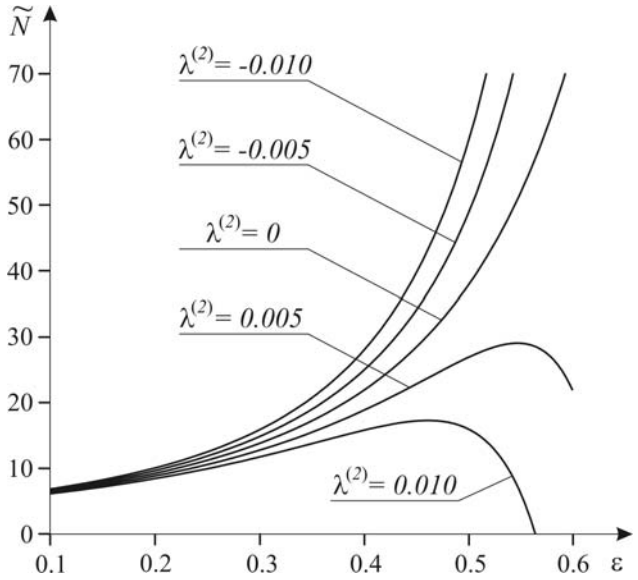

Fig.6. Dimensionless load-carrying capacity in the radial squeeze film bearing for different values of $\lambda^{(2)}$ for $n_i = 2$ (the case of the cubic type lubricant).

These plots are made for different values of $\lambda^{(n_i)}$ which indeed influence the pressure distribution and load-capacity. They are taken as the successive terms of a power series: $\lambda^{(1)}_{\max} = \pm 0.1$, $\lambda^{(2)}_{\max} = \pm 0.01$, $\lambda^{(3)}_{\max} = \pm 0.001$. This choice ensures the similar maxima of the pressure values for different fluids used for modelling of lubricant flows.

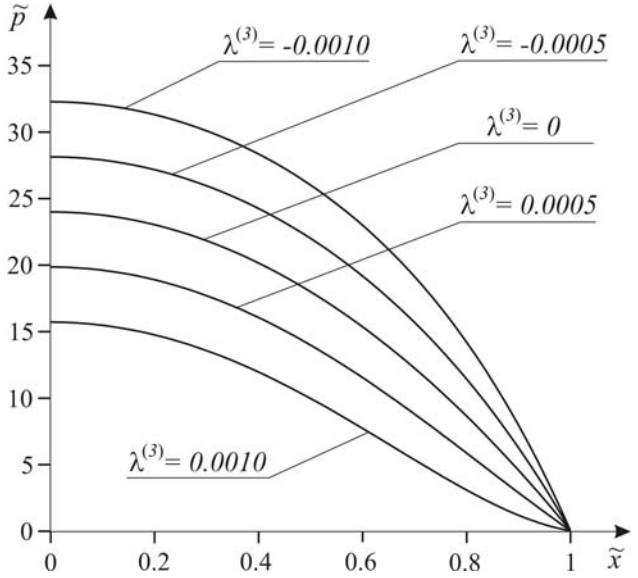

Fig.7. Dimensionless pressure distribution in the radial squeeze film bearing for $\varepsilon = 0.5$ versus different values of $\lambda^{(3)}$ for $n_i = 3$ (the case of the DeHaven-Ellis type lubricant).

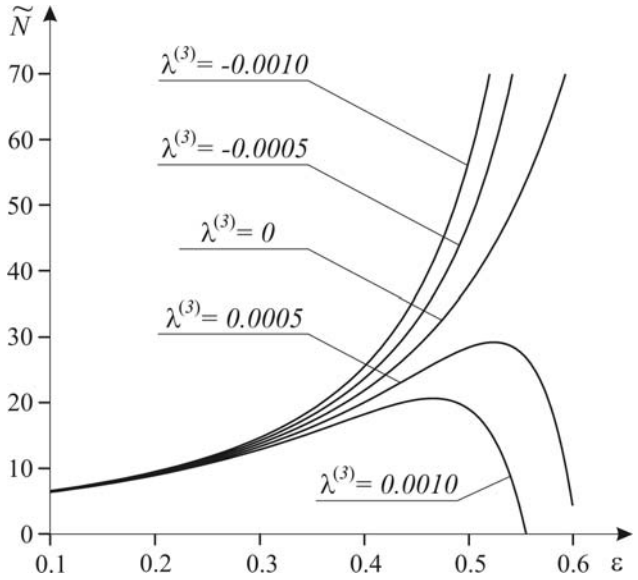

Fig.8. Dimensionless load-carrying capacity in the radial squeeze film bearing for different values of $\lambda^{(3)}$ for $n_i = 3$ (the case of the DeHaven-Ellis type lubricant).

Note that for all models of the fluids considered here the values of the material coefficients k_i have a positive sign with the exception of the Seely model for which k_i has a negative sign (see Table 1). It results from this that the plots of the pressure distribution and load-carrying capacity for the Seely fluid are placed in contrast with respect to the Newtonian fluid $\left(\lambda^{(1)} = 0\right)$.

5. Squeeze film in a spherical thrust bearing

Let us consider now a spherical squeeze film bearing shown in Fig.9.

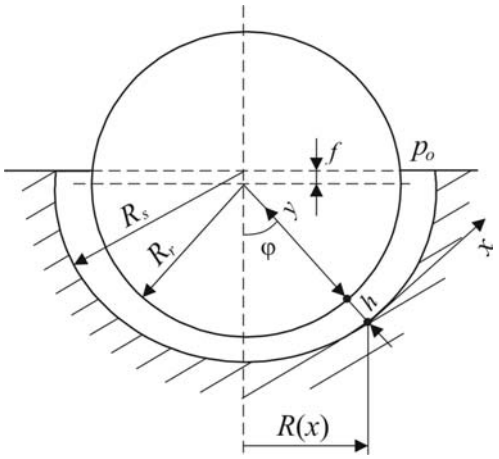

$$C = R_s - R_r,$$
$$\varepsilon(t) = \frac{f}{C},$$
$$\varphi = \frac{x}{R_r},$$
$$R = R_r \sin\varphi.$$

Fig.9. Spherical squeeze film bearing $\left(\text{for } \varphi_o = \frac{\pi}{2}\right)$.

Introducing the following parameters

$$\tilde{R}=\frac{R}{R_r}=\sin\varphi, \qquad u=\tilde{h}=\frac{h}{C}=1-\varepsilon\cos\varphi, \qquad u_o=1-\varepsilon\cos\varphi_o, \qquad e=1-\varepsilon, \qquad a=1-\varepsilon^2,$$

$$\tilde{p}=\frac{(p-p_o)}{\mu_0\dot{\varepsilon}}\left(\frac{C}{R_r}\right)^2, \quad \tilde{N}=\frac{N}{\mu_0\dot{\varepsilon}R_r^2}\left(\frac{C}{R_r}\right)^2, \quad \lambda^{(n_i)}=k_i\left(\frac{\mu_0\dot{\varepsilon}R_r}{C}\right)^{n_i}, \quad \Phi=u_o^2-e^2-2\left(u_o-e\right), \tag{5.1}$$

we will obtain the formulae for the dimensionless pressure distribution and load-carrying capacity for the spherical squeeze film bearing

$$\tilde{p}=-\frac{3}{\varepsilon}\left\{\left(\frac{1}{u_o^2}-\frac{1}{u^2}\right)+\frac{2\cdot 3^{n_i+1}\varepsilon\lambda^{(n_i)}}{(n_i+3)}\left[J^{(n_i)}(\varphi_o)-J^{(n_i)}(\varphi)\right]\right\}, \tag{5.2}$$

$$\tilde{N}=-\frac{6\pi}{\varepsilon^3}\left[\left(\ln u_o-\ln e+\frac{1}{u_o}-\frac{1}{e}-\frac{\Phi}{2u_o^2}\right)+\frac{2\cdot 3^{n_i+1}\varepsilon^3\lambda^{(n_i)}}{(n_i+3)}J_N^{(n_i)}(\varphi_o)\right] \tag{5.3}$$

where

$$J^{(n_i)}(\varphi)=\int\frac{\sin^{n_i+1}\varphi d\varphi}{u^{2n_i+3}}, \qquad J_N^{(n_i)}(\varphi_o)=\frac{1}{2}\int_0^{\varphi_o}\frac{\sin^{n_i+3}\varphi d\varphi}{u^{2n_i+3}}. \tag{5.4}$$

The expressions for $J^{(n_i)}(\varphi)$ and $J_N^{(n_i)}(\varphi_o)$ are given in the Appendix.

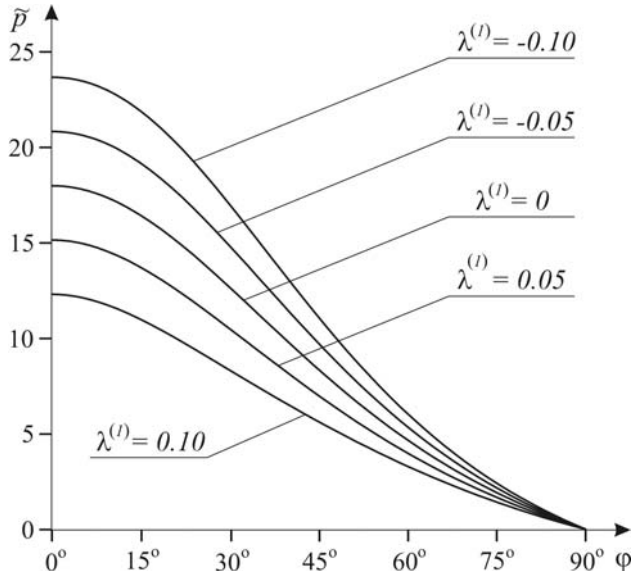

Fig.10. Dimensionless pressure distribution in the spherical squeeze film bearing for $\varepsilon=0.5$ versus different values of $\lambda^{(1)}$ for $n_i=1$ (the case of the Peek-McLean type lubricant).

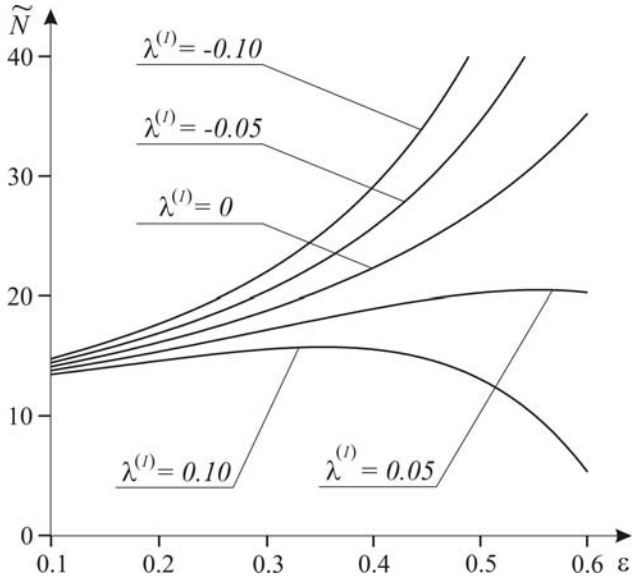

Fig.11. Dimensionless load-carrying capacity in the spherical squeeze film bearing for different values of $\lambda^{(1)}$ for $n_i = 1$ (the case of the Peek-McLean type lubricant).

The plots of the dimensionless pressure distribution and load-carrying capacity are presented for the same models as in the previous bearing case, namely in Figs 10 and 11 for the fluid of Peak-Mclean $(n_i = 1)$, in Figs 12 and 13 for one of the fluids which represent the cubic models $(n_i = 2)$ and in Figs 14 and 15 for one of DeHaven-Ellis models $(n_i = 3)$.

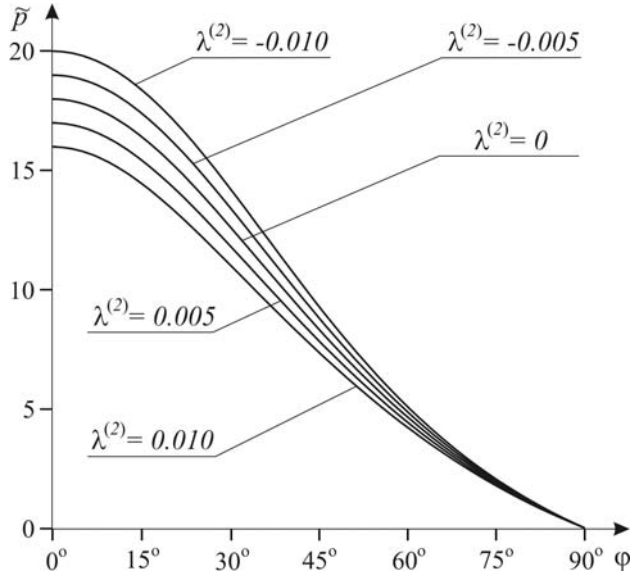

Fig.12. Dimensionless pressure distribution in the spherical squeeze film bearing for $\varepsilon = 0.5$ versus different values of $\lambda^{(2)}$ for $n_i = 2$ (the case of the cubic type lubricant).

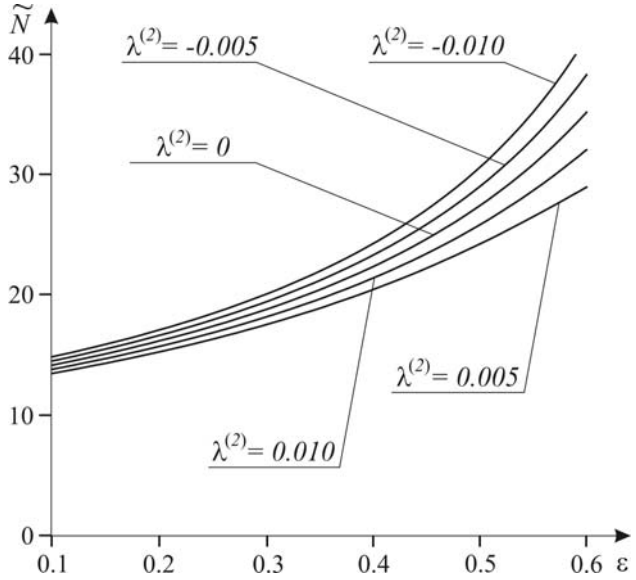

Fig.13. Dimensionless load-carrying capacity in the spherical squeeze film bearing for different values of $\lambda^{(2)}$ for $n_i = 2$ (the case of the cubic type lubricant).

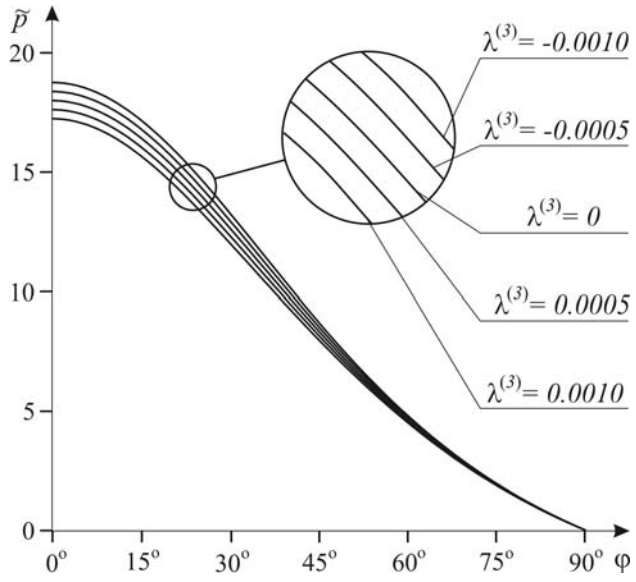

Fig.14. Dimensionless pressure distribution in the spherical squeeze film bearing for $\varepsilon = 0.5$ versus different values of $\lambda^{(3)}$ for $n_i = 3$ (the case of the DeHaven-Ellis type lubricant).

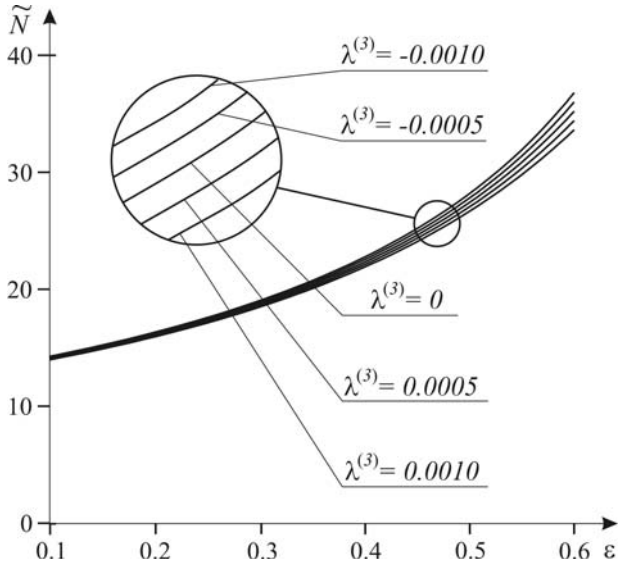

Fig.15. Dimensionless load-carrying capacity in the spherical squeeze film bearing for different values of $\lambda^{(3)}$ for $n_i = 3$ (the case of the DeHaven-Ellis type lubricant).

Note that these plots are generally similar to the plots of the previous bearing case, but for $n_i = 3$ the group of plots both for the pressure distribution and load-carrying capacity are more concentrated.

6. Results and discussion

According to the above analysis, the performance of non-Newtonian curved squeeze films is influenced by three parameters: the first two are geometric parameters and the third one is a rheological parameter. The geometric parameters R and h, or in a dimensionless form $\tilde{R}$ and $\tilde{h}$, define the curved shape of the bearing gap; if $\tilde{R} = \tilde{x}$ and $\tilde{h} = e(t)$ they generate a circular (radial) squeeze film, but if $\tilde{R} = \sin\varphi$ and $\tilde{h} = u = 1 - \varepsilon\cos\varphi$ they generate a spherical squeeze films. The rheological nonlinear parameter $\lambda^{(n_i)}$ characterizes the non-Newtonian behaviour of the DeHaven fluid model or other similar models of fluids. It is applicable to dilatant fluids for $\lambda^{(n_i)} < 0$, to Newtonian fluids for $\lambda^{(n_i)} = 0$ and to pseudo-plastic fluids for $\lambda^{(n_i)} > 0$.

For $\lambda^{(n_i)} = 0$ and $\tilde{R} = \tilde{x}$: this is a Newtonian radial squeeze film as in Hamrock [44], but for $\tilde{R} = \sin\varphi$ this is a Newtonian spherical squeeze film as in Walicki [10]. For $\lambda^{(n_i)} \neq 0$ and $\tilde{R} = \tilde{x}$ or $\tilde{R} = \sin\varphi$: it is a non-Newtonian curved circular or spherical squeeze film (present study).

Figures 3-8 present the film pressures and the load capacities for a circular squeeze film, respectively. The film pressure $\tilde{p}$ is presented as a function of the radial coordinate $\tilde{x}$ for the squeezing ratio $\varepsilon = 0.5$ for different values of $\lambda^{(n_i)}$ $(n_i = 1,2,3)$, but the load capacity is presented as a function of the squeezing ratio ε for different values of $\lambda^{(n_i)}$. It is observed that the effects of the pseudo-plasticity $\left(\lambda^{(n_i)} > 0\right)$ decrease the film pressure and load capacity with respect to the case of a Newtonian lubricant but the effects of the dilatancy $\left(\lambda^{(n_i)} < 0\right)$ increase both the mechanical parameters. The differences between these parameters for the cases of non-Newtonian and Newtonian lubricants are considerable. With the increase of n_i (index of the model non-linearity) the film pressures and load capacities decrease considerably.

Figures 10-15 present the film pressures and load capacities for a spherical squeeze film, respectively. The film pressure $\tilde{p}$ is presented as a function of the spherical coordinate φ for the

eccentricity ratio $\varepsilon = 0.5$ also for different values of $\lambda^{(n_i)}$, whereas the load capacity is presented as a function of the eccentricity ratio ε for different values of $\lambda^{(n_i)}$. It may be observed that generally both the phenomena (pressure and load capacity) change similarly as in the previous case, but the changes are smaller. The values of both the mechanical parameters are smaller compared to the previous case; it is compatible with the study made by Lin *et al.* [18] for the Rabinowitsch fluid (our case $n_i = 2$).

7. Conclusion

Basing on the non-Newtonian lubricant model we develop the study of squeeze film bearing lubricated by the DeHaven fluid or the other similar models of fluids. The modified non-linear Reynolds equation is derived and its solution is obtained by the method of successive approximations. Two squeeze film bearings are considered: radial (circular) and spherical. Dimensionless pressures and load capacities are calculated and presented graphically for both the bearings. Higher pressures and load capacities are obtained for bearings lubricated with dilatant lubricants $\left(\lambda^{(n_i)} < 0\right)$, but the pseudo-plastic lubricants $\left(\lambda^{(n_i)} > 0\right)$ yield reverse results. The values of the pressures and load capacities for the same values of the rheological parameters $\lambda^{(n_i)}$ are higher for the case of a radial bearing compared to these ones for the case of a spherical bearing.

Nomenclature

$\boldsymbol{A}_1$ – the first Rivlin-Ericksen kinematic tensor
C_1 – constant of integration
$F^{(n_i)}(x,t)$ – auxiliary function for the pressure distribution
h, $h(x,t)$ – clearance thickness
$I(x,t)$ – function presented Newtonian part of the pressure distribution
$J^{(n_i)}(x,t)$ – function presented pseudoplastic correction in the pressure distribution
k, k_i – pseudo-plasticity coefficients
N – load-carrying capacity
n, n_i – exponents of pseudo-plasticity
p – pressure
$R, R(x)$ – local radius of the lower bearing surface
r – radius
r, z – cylindrical coordinates
$\boldsymbol{T}$ – shear stress tensor
υ_x, υ_y – velocity components
x, y – orthogonal coordinate
$\varepsilon(t)$ – squeezing ratio or eccentricity
$\boldsymbol{\Lambda}$ – extra stress tensor
ϑ – angular coordinate
μ_0 – coefficient of shear viscosity
μ_∞ – final shear viscosity
μ – plastic viscosity
ρ – fluid density
τ – shear stress

Appendix

The expressions for $J^{(1)}(\varphi)$ and $J_N^{(1)}(\varphi_o)$

$$J^{(1)}(\varphi)=-\frac{\sin\varphi}{4\varepsilon u^4}+\frac{\sin\varphi}{12\varepsilon a u^3}+\frac{\left(2+3\varepsilon^2\right)\sin\varphi}{24\varepsilon a^2u^2}+\frac{\left(2+13\varepsilon^2\right)\sin\varphi}{24\varepsilon a^3u}+$$
$$+\frac{\left(4+\varepsilon^2\right)}{4a^3}\frac{1}{\sqrt{a}}\arctan\left(\frac{\sqrt{a}\tan\frac{\varphi}{2}}{e}\right),$$

$$J_N^{(1)}(\varphi_o)=\frac{a\sin\varphi_o}{8\varepsilon^3u_o^4}-\frac{3\sin\varphi_o}{8u_o^3\varepsilon^3}+\frac{\left(6-5\varepsilon^2\right)\sin\varphi_o}{16au_o^2\varepsilon^3}+$$
$$-\frac{\left(2-5\varepsilon^2\right)\sin\varphi_o}{16\varepsilon^3a^2u_o}+\frac{6\varepsilon^4}{\sqrt{a}}\arctan\left(\frac{\sqrt{a}\tan\frac{\varphi_o}{2}}{e}\right).$$

The expressions for $J^{(2)}(\varphi)$ and $J_N^{(2)}(\varphi_o)$

$$J^{(2)}(\varphi)=\frac{1}{6\varepsilon^3}\left(\frac{a}{u^6}-\frac{12}{5u^5}+\frac{3}{2u^4}\right),$$

$$J_N^{(2)}(\varphi_o)=\frac{1}{2\varepsilon^5}\left[\left(-\frac{a^2}{6u_o^6}+\frac{4a}{5u_o^5}-\frac{3-\varepsilon^2}{2u_o^4}+\frac{4}{3u_o^3}-\frac{1}{2u_o^2}\right)+\right.$$
$$\left.-\left(-\frac{a^2}{6e^6}+\frac{4a}{5e^5}-\frac{3-\varepsilon^2}{2e^4}+\frac{4}{3e^3}-\frac{1}{2e^2}\right)\right].$$

The expressions for $J^{(3)}(\varphi)$ and $J_N^{(3)}(\varphi_o)$

$$J^{(3)}(\varphi)=\frac{a\sin\varphi}{8u^8\varepsilon^3}-\frac{17\sin\varphi}{56u^7\varepsilon^3}-\frac{7\sin\varphi}{48u^6\varepsilon^3}+\frac{115\sin\varphi}{336au^6\varepsilon^3}+\frac{253\sin\varphi}{336a^2u^5\varepsilon^3}+$$
$$-\frac{1271\sin\varphi}{1680au^5\varepsilon^3}+\frac{759\sin\varphi}{448a^3u^4\varepsilon^3}-\frac{7157\sin\varphi}{3360a^2u^4\varepsilon^3}+\frac{83\sin\varphi}{192au^4\varepsilon^3}+\frac{253\sin\varphi}{64a^4u^3\varepsilon^3}+$$
$$-\frac{6691\sin\varphi}{1120a^3u^3\varepsilon^3}+\frac{4519\sin\varphi}{2240a^2u^3\varepsilon^3}+\frac{1265\sin\varphi}{128a^5u^2\varepsilon^3}-\frac{2237\sin\varphi}{128a^4u^2\varepsilon^3}+\frac{36909\sin\varphi}{4480a^3u^2\varepsilon^3}+$$
$$-\frac{83\sin\varphi}{128a^2u^2\varepsilon^3}+\frac{3795\sin\varphi}{128a^6u\varepsilon^3}-\frac{7723\sin\varphi}{128a^5u\varepsilon^3}+\frac{4693\sin\varphi}{128a^4u\varepsilon^3}-\frac{26791\sin\varphi}{4480a^3u\varepsilon^3}+$$
$$-\frac{\sin\varphi}{3au^6\varepsilon}-\frac{11\sin\varphi}{15a^2u^5\varepsilon}-\frac{33\sin\varphi}{20a^3u^4\varepsilon}+\frac{5\sin\varphi}{12a^2u^4\varepsilon}-\frac{77\sin\varphi}{20a^4u^3\varepsilon}+\frac{39\sin\varphi}{20a^3u^3\varepsilon}+$$
$$-\frac{77\sin\varphi}{8a^5u^2\varepsilon}+\frac{147\sin\varphi}{20a^4u^2\varepsilon}+-\frac{5\sin\varphi}{8a^3u^2\varepsilon}-\frac{231\sin\varphi}{8a^6u\varepsilon}+\frac{119\sin\varphi}{4a^5u\varepsilon}-\frac{231\sin\varphi}{40a^4u\varepsilon}+$$
$$+\left(\frac{3795}{128a^6\varepsilon^4}-\frac{2247}{32a^5\varepsilon^4}+\frac{3465}{64a^4\varepsilon^4}-\frac{455}{32a^3\varepsilon^4}+\frac{83}{128a^2\varepsilon^4}-\frac{231}{8a^6\varepsilon^2}+\right.$$
$$\left.+\frac{315}{8a^5\varepsilon^2}-\frac{105}{8a^4\varepsilon^2}+\frac{5}{8a^3\varepsilon^2}\right)\frac{2}{\sqrt{a}}\arctan\left(\frac{\sqrt{a}\tan\frac{\varphi}{2}}{e}\right),$$

$$J_N^{(3)}(\varphi_o) = \frac{a^3 \sin\varphi_o}{16u_o^8\varepsilon^7} - \frac{7a^2 \sin\varphi_o}{16u_o^7\varepsilon^7} + \frac{101a \sin\varphi_o}{96u_o^6\varepsilon^7} + \frac{25a^2 \sin\varphi_o}{96u_o^6\varepsilon^7}$$
$$- \frac{85\sin\varphi_o}{96u_o^5\varepsilon^7} - \frac{125a\sin\varphi_o}{96u_o^5\varepsilon^7} + \frac{337\sin\varphi_o}{192u_o^4\varepsilon^7} + \frac{\sin\varphi_o}{128au_o^4\varepsilon^7}$$
$$+ \frac{163a\sin\varphi_o}{384u_o^4\varepsilon^7} - \frac{163\sin\varphi_o}{128u_o^3\varepsilon^7} + \frac{7\sin\varphi_o}{384a^2u_o^3\varepsilon^7} - \frac{11\sin\varphi_o}{192au_o^3\varepsilon^7}$$
$$+ \frac{93\sin\varphi_o}{256u_o^2\varepsilon^7} + \frac{35\sin\varphi_o}{768a^3u_o^2\varepsilon^7} - \frac{119\sin\varphi_o}{768a^2u_o^2\varepsilon^7} + \frac{47\sin\varphi_o}{256au_o^2\varepsilon^7} + \frac{35\sin\varphi_o}{256a^4u_o\varepsilon^7}$$
$$- \frac{385\sin\varphi_o}{768a^3u_o\varepsilon^7} + \frac{511\sin\varphi_o}{768a^2u_o\varepsilon^7} - \frac{93\sin\varphi_o}{256au_o\varepsilon^7} + \left(\frac{35}{256\varepsilon^8} + \frac{35}{256a^4\varepsilon^8} + \right.$$
$$\left. - \frac{35}{64a^3\varepsilon^8} + \frac{105}{128a^2\varepsilon^8} - \frac{35}{64a\varepsilon^8} \right) + \frac{2}{\sqrt{a}} \arctan\left(\frac{\sqrt{a}\tan\frac{\varphi_o}{2}}{e} \right).$$

References

[1] Walicka A. (1994): *Micropolar Flow in a Slot Between Rotating Surfaces of Revolution.* – Zielona Góra: TU Press.

[2] Walicki E. and Walicka A. (1998): *Mathematical modelling of some biological bearings.* – Smart Materials and Structures, Proc. 4th European and 2nd MiMR Conference, Harrogate, UK, 6-8 July 1998, pp.519-525.

[3] Khonsari M.M. and Dai F. (1992): *On the mixture flow problem in lubrication of hydrodynamic bearing: small solid volume fraction*. – STLE Trib. Trans., vol.35, No.1, pp.45-52.

[4] Lipscomb C.C. and Denn M.M. (1984): *Flow of Bingham fluids in complex geometries*. – J. Non-Newt. Fluid Mech., vol.14, No.3, pp.337-349.

[5] Dorier C. and Tichy J. (1992): *Behaviour of a Bingham-like viscous fluid in lubrication flows*. – J. Non-Newt. Fluid Mech., vol.45, No.3, pp.291-350.

[6] Wada S. and Hayashi H. (1971): *Hydrodynamic lubrication of journal bearings by pseudo-plastic lubricants.* Pt 1, Theoretical Studies, Pt 2, Experimental Studies. – Bull. JSME, vol.14, No.69, pp.268-286.

[7] Swamy S.T.N., Prabhu B.S. and Rao B.V.A. (1975): *Stiffness and damping characteristics of finite width journal bearing with a non-Newtonian film and their application to instability prediction.* – Wear, vol.32, pp.379-390.

[8] Rajalingham C., Rao B.V.A. and Prabu S. (1978): *The effect of a non-Newtonian lubricant on piston ring lubrication.* – Wear, vol.50, pp.47-57.

[9] Walicka A. (2002): *Rotational Flows of Rheologically Complex Fluids in Thin Channels* (in Russian). – Zielona Góra: University Press.

[10] Walicki E. (2005): *Rheodynamics of Slide Bearings Lubrication* (in Polish). – Zielona Gora: University Press.

[11] Kraemer E.O. and Williamson, R.V. (1929): *Internal friction and the structure of „solvated" colloids*. – J. Rheology, vol.1, No.1, pp.76-92.

[12] Rabinowitsch B. (1929): *Über die Viskosität und Elastizität von Solen* (*On the viscosity and elasticity of sols*). – Zeit. Phys. Chem., A145, pp. 1-26.

[13] Rotem Z. and Shinnar R. (1961): *Non-Newtonian flow between parallel boundaries in linear movements.* – Chem. Eng. Sie., vol.15, pp.130-143.

[14] Sharma S.C., Jain S.C. and Sah P.L. (2000): *Effect of non-Newtonian behaviour of lubricant and bearing flexibility on the performance of slot-entry journal bearing*. – Tribology Int. vol.33, pp.507-517.

[15] Singh U.P., Gupta R.S. and Kapur V.K. (2011): *On the steady performance of hydrostatic thrust bearing: Rabinowitsch fluid model*. – Tribology Transactions, vol.54, pp.723-729.

[16] Hashimoto H. and Wada S. (1986): *The effects of fluid inertia forces in parallel circular squeeze film bearing lubricated with pseudoplastic fluids*. – J. Tribology, vol.108, pp.282-287.

[17] Lin J.-R. (2012): *Non-Newtonian squeeze film characteristics between annular disks: Rabinowitsch fluid model.* – Tribology Int. 52, pp.190-194.

[18] Lin J.-R., Chu L.-M., Hung C.-R., Lu, R.-F. and Lin M.-C. (2013): *Effects of non-Newtonian rheology on curved circular squeeze film: Rabinowitsch fluid model*. – Z. Naturforsch., vol.68a, pp.291–299.

[19] Walicka, A., Walicki, E. and Ratajczak, M. (1999): *Pressure distribution in a curvilinear thrust bearing with pseudo-plastic lubricant*. – Appl. Mech. Enging. vol.4 (sp. Issue), pp.81-88.

[20] Walicka A., Walicki E. and Ratajczak M. (2000): *Rotational inertia effects in a pseudo-plastic fluid flow between non-coaxial surfaces of revolution*. – Proc. 4th Minsk Int. Heat Mass Transfer Forum (May 22-27, 2000 Minsk Belarus), pp.19-29.

[21] Ratajczak M., Walicka A. and Walicki E. (2006): *Inertia effects in the curvilinear thrust bearing lubricated by a pseudo-plastic fluid of Rotem-Shinnar*. – Problems of Machines Exploitation, vol.44, pp.159-170.

[22] Walicka A. and Walicki E. (2010): *Performance of the curvilinear thrust bearing lubricated by a pseudo-plastic fluid of Rotem-Shinnar*. – Int. J. Appl. Mech. Enging, vol.15, no.3, pp.895-907.

[23] DeHaven E.S. (1959): *Control valve design for viscous pseudoplastic fluids*. – Ind. Eng. Chem., vol.51, No.7, pp.63A-66A.

[24] Ree T and Eyring H. (1995): *Theory of non-Newtonian flow II, Solution system of high polymers*. –J. Appl. Physics, vol.26, No.7, pp.793-809.

[25] Meter D.M. (1964): *Tube flow of non-Newtonian polymer solutions: Part II. Turbulent flow*. – AIChE Journal. vol.10, pp.881-884.

[26] Ellis S.B. (1927): Thesis, Lafayette College, Pa. Citted in: Matsuhisa S., Bird R.B. (1965): *Analytical and numerical solutions for laminar flow of the non-Newtonian Elis fluid*. - AiChE Journal, vol.11, No.4, pp.588-595.

[27] Reiner M. (1960): *Deformation, Strain and Flow*. – London: H.K. Lewis & Co..

[28] Philippoff W. (1942): *Viscosität der Kolloide*. – Dresden: T. Steinkopff.

[29] Peek R.L. and McLean S. (1931): *Some Physical Concepts in Theories of Plastic Flow*. – J. Rheol. vol.2, pp.377-384.

[30] Seely G.R. (1964): *Non-Newtonian viscosity of polybutadiene solutions*. – AIChE Journal, vol.10, No.1, pp.56-60.

[31] Ratajczak M., Walicka A., Walicki E. and Ratajczak P. (2006): *Rheodynamics of lubrication of curvilinear thrust bearings with Ellis pseudoplastic fluid*. – Scientific Problems of Machines Operation and Maintenance, vol.41, No.2, pp.147-158.

[32] Walicka A. (2017): *Rheology of Fluid in Mechanical Engineering.* – Zielona Góra: University Press.

Received: March 13, 2017

Revised: May 22, 2017